Eur. Phys. J. B **3**, 189–196 (1998)

THE EUROPEAN PHYSICAL JOURNAL B

Transfer of smectic films to a solid substrate by the method of Maclennan

I.V. Chikina[1,a], N. Limodin[2], A. Langlois[2], M. Brazovskaia[2], C. Even[2], and P. Pieranski[2,b]

[1] Laboratoire Léon Brillouin CEA Saclay-CNRS, 91191 Gif-sur-Yvette, France
[2] Laboratoire de Physique des Solides, Université Paris-Sud, Bâtiment 510, 91405 Orsay Cedex, France

Received: 25 November 1997 / Received in final form: 30 January 1998 / Accepted: 9 March 1998

Abstract. Free-standing smectic films are transferred onto a solid substrate by the method of Maclennan. When examined with an atomic force microscope, the transferred films show a large number of small holes. In order to explain the genesis of these defects, the transfer process is analysed both experimentally and theoretically. In particular, shapes of free films spanned between the flat substrate and a circular frame are calculated and it is shown that during the transfer process films are submitted to an increase of their surface area. During experimental studies of the transfer process, stable and unstable forms of the catenoid-shaped free films, spanned between the substrate and the circular frame, are observed. Their existence is explained theoretically.

PACS. 61.30.-v Liquid crystals – 68.15.+e Liquid thin films

1 Introduction

Smectic liquid crystals form easily the so-called free standing films which attracted much attention because of their remarkable structural features and unusual physical properties [1]. In particular, it has been shown that it is possible to draw films of perfectly uniform thickness that can range between two and several thousands molecular layers. Maclennan *et al.* [2] proposed a method of transfer of such highly perfect films onto a solid substrate with the aim to make them more convenient for applications. This method uses the possibility of inflating smectic films as it has been shown for the first time by Oswald [3]. It consists in disposing the substrate (a mica sheet or a glass plate) close to the smectic bubble in a way that it touches the substrate and adheres to it.

In the present work (Sect. 2), we report on first AFM studies of films transferred by the Maclennan method and point out that during the transfer process many tiny holes are open in the film. As a possible explanation of the genesis of these defects we propose an abrupt increase in the surface area of the film when it adheres to the substrate. In Section 3, we calculate the surface areas S_b and S_a of the film before and after the transfer and show that the difference $\Delta S = S_a - S_b$ is positive and increases as a function of the distance h between the flat film and the substrate.

In the calculation of the surface area of the transferred film, one has to take into account two parts: the flat film of radius r_0 transferred on the substrate (its surface area is obviously πr_0^2) and the curved free-standing film spanned between the rim of the hole and the surface of the substrate (Fig. 3). We calculate the shape and the surface area of this free film in two limits. In the limit of zero pressure, the film has the shape of the minimal surface of revolution – the catenoid. In agreement with previous results of Cryer and Steen [4] we show theoretically that for given distance h, two catenoid-shaped films can be spanned between the hole and the substrate: one of them is stable and the other one unstable. In Section 2 we show that both types of catenoid can be realised experimentally. The second limit we consider corresponds to a constant pressure Δp such that the top of the spherical smectic bubble just touches the substrate. In this case, the free film spanned between the hole and the substrate has, after the transfer, the shape of the surface of revolution of a constant mean curvature. We calculate this shape and the corresponding surface area numerically.

2 Experimental

2.1 Film transfer

The experimental set-up we used for the transfer of the free-standing films was inspired by the one of Maclennan (Fig. 1a). The smectic film is suspended on a circular aperture of radius R open in the cover of a small tight

[a] *Current address*: Institute of Microelectronics Technology of Russian Academy of Science, 142432 Chernogolovka, Russia.
[b] e-mail: `pawel@lps.u-psud.fr`

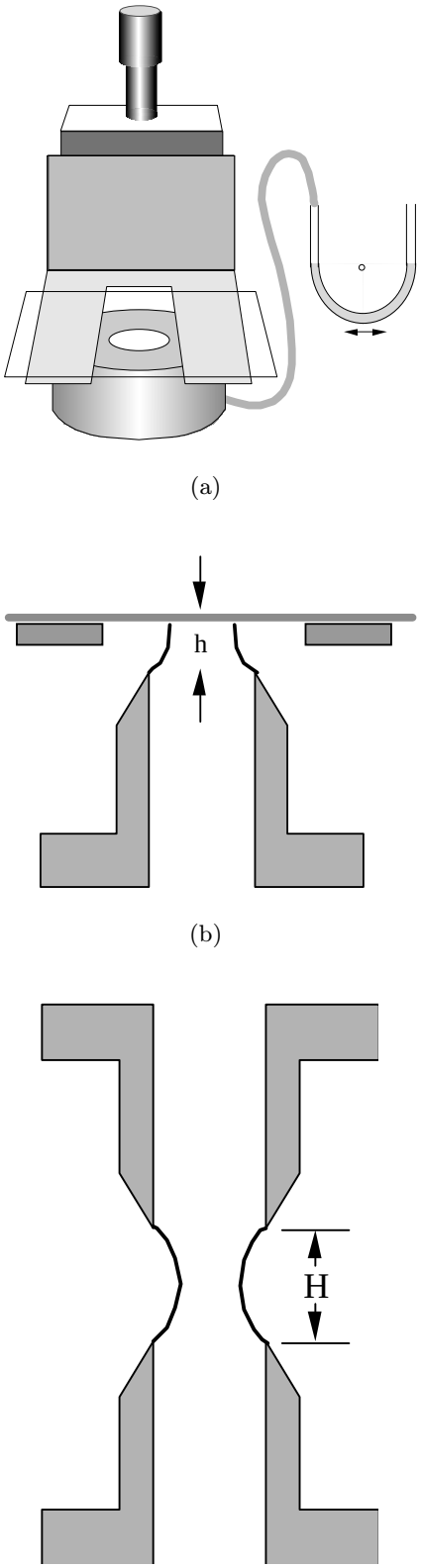

Fig. 1. Experimental set-up: (a) for the film transfer, (b) for the study of the half-catenoid, (c) for the study of the whole catenoid.

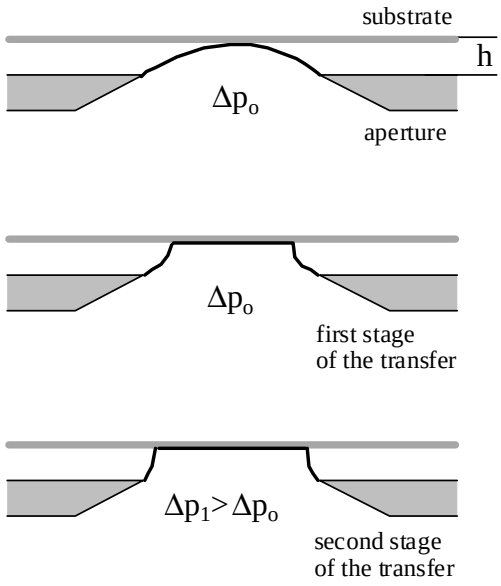

Fig. 2. Transfer process.

box. The film is drown using a razor blade which cutting edge is wet with the liquid crystal. The razor blade is moved slowly across the hole by means of a translation stage. This operation is made under a reflecting microscope in order to monitor the thickness and the texture of the film. The pressure in the box is controlled simply using a U-shaped tube filled partially with water. Tilting of the tube displaces the water column in it and results in a change of the pressure inside the box. The substrate (a freshly cleaved mica sheet or a microscope cover glass) is supported by a fork-shaped part attached to a translation stage which allows to control the distance h with the accuracy of 0.02 mm.

The smectic liquid crystals used in experiments were either the commercial mixture SCE4 (from BDH) possessing the SmC* phase at room temperature or 8CB having the SmA phase at room temperature. The first choice of the mesophase was determined by the initial aim of our AFM studies – detection of the topography of SmC* films due to the distortion in the director field **c**. Such a distorsion can occur spontaneously as it has been shown by Maclennan [5] or by Demikhov and Stegemeyer [6].

2.1.1 First stage of the transfer

In order to transfer the film onto the substrate we used two methods (Fig. 2). In the first one, the film is slightly inflated by a small constant pressure Δp_0. Subsequently, the substrate is slowly lowered using the translation stage until it touches the top of the smectic bubble. The second method is inverse: the distance h is kept fixed and the pressure is raised slowly until the top of the inflated smectic film touches the substrate. Obviously, the height h at which the contact between the smectic bubble and the substrate is established depends on the pressure

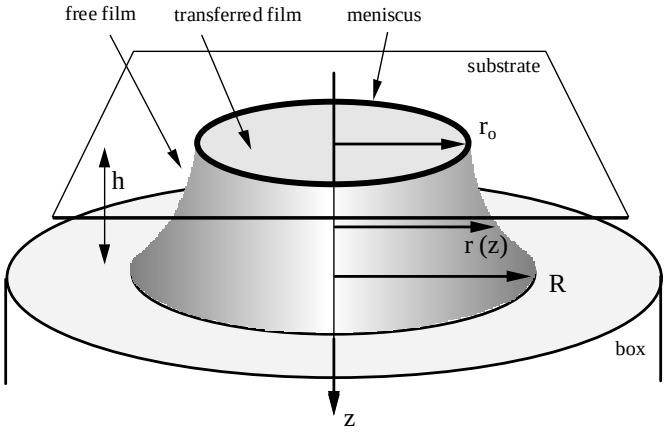

Fig. 3. Configuration resulting from the first stage of the transfer.

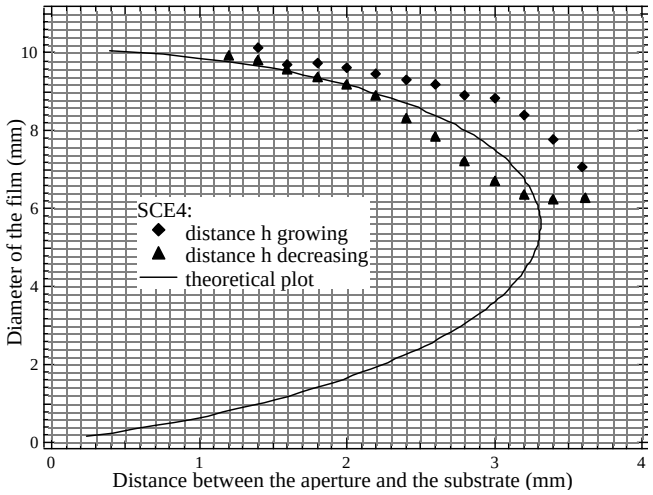

Fig. 4. Diameter of the transfered film $2r_0$ *versus* the distance h between the aperture and the substrate. The time laps between measurements is of the order of a few seconds. The hysteresis is due to the relaxation time.

Δp. This function $\Delta p(h)$ is calculated in Section 3 (Eqs. (6, 7)).

Once the first contact between the film and the substrate is realised, the film adheres to the substrate extremely rapidly (in about a few milliseconds) and as a result one obtains the configuration depicted in Figure 3: a disc-shaped area of radius r_0 of the substrate covered with the transferred smectic film and a free-standing film spanned between the substrate and the circular aperture. Let us emphasise that after the first stage of the transfer, a meniscus forms between the substrate and the free film. It is well visible as a ring of radius r_0 and of thickness Δr of about 0.1 mm. Due to the presence of this meniscus, the contact angle between the free film and the substrate is $\pi/2$. Knowing the contact angle, the radius R of circular aperture and the pressure Δp, the shape of the free film and, in particular, its radius r_0 at the substrate are calculated as a function of the distance h in Section 2.1.

2.1.2 Second stage of the transfer

It results from the theoretical analysis that the shape of the free film depends on the distance h and the pressure difference Δp. For this reason, as mentioned already in [2], the spreading of the film can be continued either by rising the pressure Δp or by decreasing the distance h. It is important to note however that in this second stage of the transfer process, the transferred film is much thicker than the free film. Indeed, when the pressure Δp or the distance h undergo a step-like change, the radius r_0 of the meniscus increases slowly toward a new equilibrium value. During this motion, the meniscus wets the clean substrate and lefts behind a wetting film which thickness depends now mainly on the structure and the velocity of the meniscus.

2.1.3 Half-catenoid-shaped free films

In order to study in more details the motion of the meniscus we modified the set-up as follows (Fig. 1b). The box with the circular aperture is replaced by a circular vertical tube of diameter 1 cm. The upper end of the tube is machined in order to obtain a sharp rim. This rim is wet with a small amount of the liquid crystal and the substrate plate is lowered until it touches the rim. In the absence of the pressure, when the substrate is slowly raised up, a half-catenoid- shaped film forms between the rim and the substrate. The film is observed with a TV camera either from the top or from the side. In the first case, one sees the circular meniscus of radius r_0 which connects the film to the substrate. In the second case, the film profile $r(z)$ is well visible (see Fig. 7).

The radius r_0 of the meniscus was measured as a function of the distance h. In this first experiment, the time laps between consecutive measures was of the order of a few seconds. The resulting plot r_0 *versus* h is shown in Figure 4. The first remarkable feature of the first plot is the hysteresis: the values of the radius obtained during the increase of the distance h are larger than those obtained during the decrease of h. The difference Δr_0 grows with h. The reason of this hysteresis is the dynamics of the meniscus. When h undergoes a step-like change Δh, the meniscus evolves slowly toward its new equilibrium value. As shown in Figure 6, the characteristic time of this relaxation process is usually of the order of about ten seconds but it grows with h. The divergence of the relaxation time is related to the second remarkable result of this experiment; for distances h larger than $h^* = 3.3$ mm, the catenoid loses its stability. The corresponding critical radius r_0^* is about 2.7 mm. In practice, the loss of the stability means that if h is set at a value larger than h^* and one waits long enough, the radius r_0 of the catenoid becomes less than r_0^* and goes to zero. As a result, the free film is detached from the substrate. We found however that this collapse of the catenoid is not inevitable. When the radius r_0 gets smaller than r_0^*, one can decrease

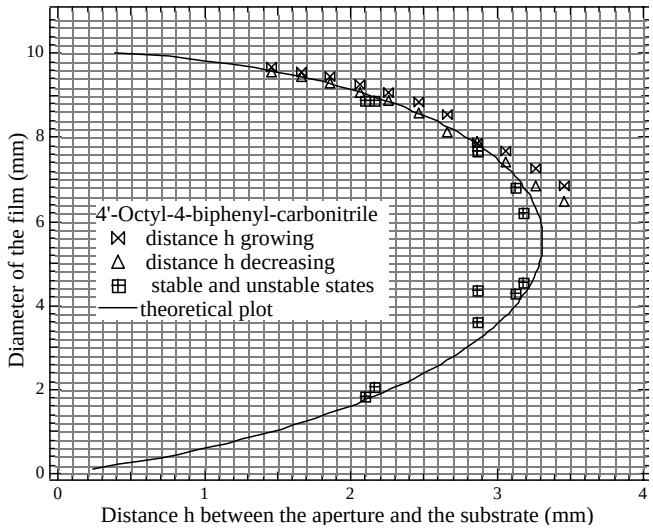

Fig. 5. Diameter of the transfered film $2r_0$ *versus* the distance h between the aperture and the substrate. The time laps between measurements has been adjusted in order to get equilibrium configuration of the meniscus. The points on the lower branch correspond to the unstable form of the catenoid.

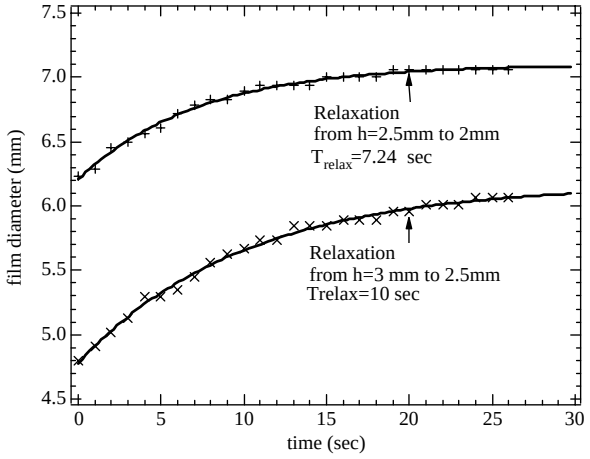

Fig. 6. Relaxation process: motion of the meniscus on the substrate plate after a change of the distance h.

rapidly the distance h and then, by a permanent (manual) control of h, stabilise dynamically the catenoid. In such a way we obtained a series of points located on the lower branch of the plot in Figure 5. These points represent unstable states corresponding to a maximum of the energy $E(r_0)$ of the free film with respect to variations of the radius r_0. In spite of that, the free film in these unstable states can always be considered as a minimal surface with respect to all infinitesimal perturbations conserving the radii R and r_0. The points situated on the upper branch of the plot in Figure 5 (the hysteresis is suppressed now thanks to a sufficient time delay between measures) correspond to the minimum of the film energy with respect to variations of r_0. In general, for each distance $h < h^*$, two catenoids, one stable and the other one unstable, can

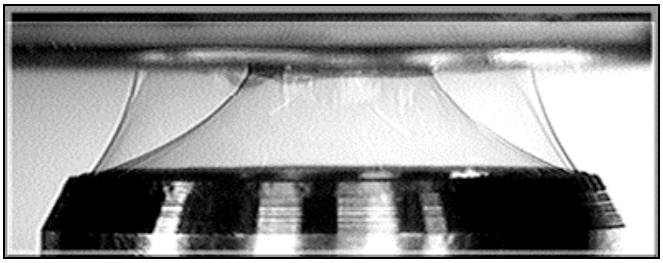

Fig. 7. Superposition of photographs of the stable and unstable forms of the catenoid corresponding to the same distance h.

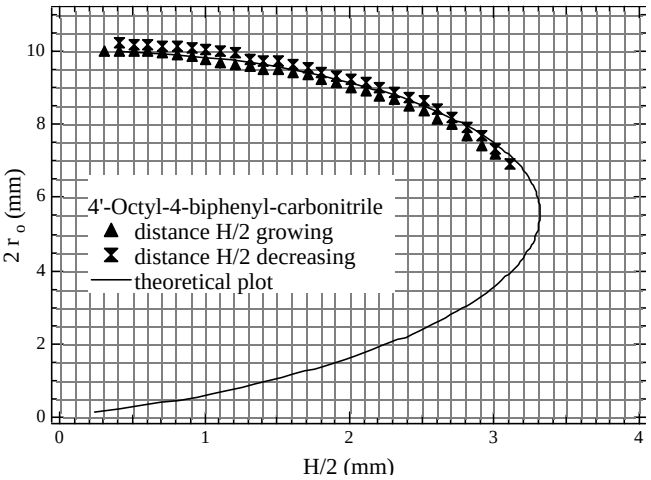

Fig. 8. Diameter *versus* height measured for the whole catenoid.

be spanned between the circular aperture and the substrate. This is illustrated in Figure 7 showing a superposition of photographs of these stable and unstable forms of the catenoid for $h = 2$ mm. The depth of the minimum (stable states) and the height of the maximum (unstable states) can be analysed qualitatively from the dynamical behaviour. From the divergence of the relaxation time one can deduce that the depth and height of these extrema decrease as a function of h and vanish at $h = h^*$, where, for $r_f = r_f^*$, the function $E(r_0)$ has only an inflexion point of zero slope. The divergence of the relaxation time in the limit $h \to h^*$ described above can be seen as a critical slowing down of a diffusive mode. The mode corresponding to changes in the radius r_0 is diffusive because of the viscous friction during the motion of the meniscus on the substrate.

2.1.4 Catenoid-shaped free films

In the last series of experiments, we replaced the flat substrate by a circular frame, identical to the lower one as shown in Figure 1c. In this case, only the stable form of the catenoid has been observed and its radius r_0 at the half-height $h = H/2$ was measured as a function of the distance H between frames (Fig. 8). The unstable form

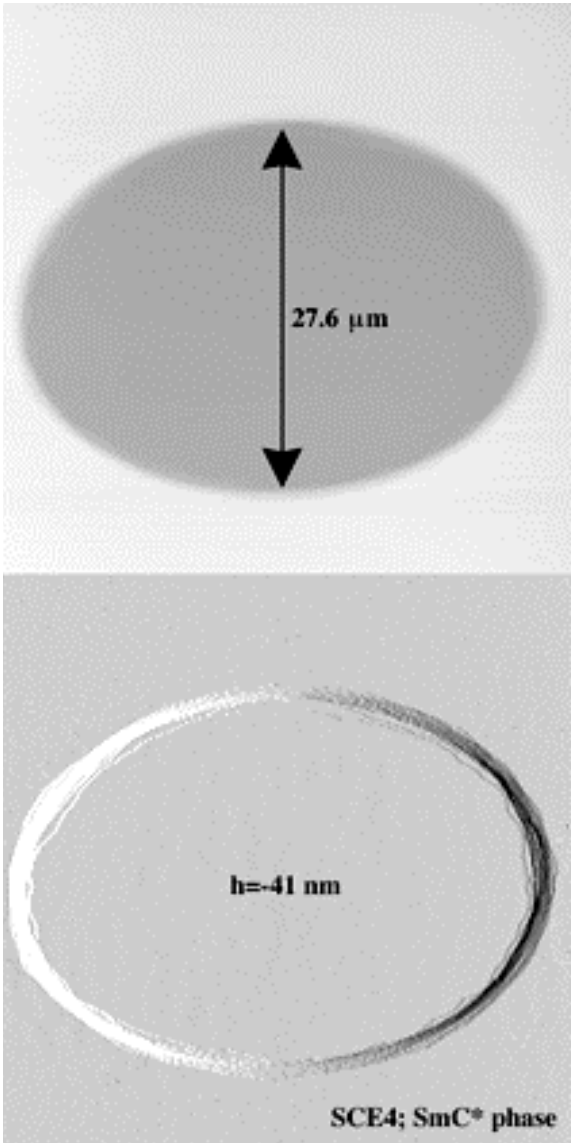

Fig. 9. Typical AFM image of holes in a SCE4 film.

is now impossible to control manually because, in the absence of the viscous drag on the substrate plate, changes in the radius r_0 are very rapid and, in the case of the stable form, they correspond to an oscillatory mode – the fundamental eigenmode of vibrations of the minimal surface. Its eigenfrequency is now expected to vanish in the limit $H/2 \to h^*$. The study of this soft mode is presented in the accompanying paper [8].

2.2 AFM study of films transferred by the Maclennan method

The AFM study of films transferred by the Maclennan method was the initial aim of the present work. In particular, we were interested in the topography characteristic of $\pm 2\pi$ disclinations. For this purpose, the films were drawn under a polarising microscope and transferred (by the first stage of the process under a constant pressure Δp_0) onto a mica sheet when they presented several disclinations. The thickness of free films before the transfer ranged between 5 and 30 layers. The mica sheets with the smectic films were examined by means of the Nanoscope III atomic force microscope.

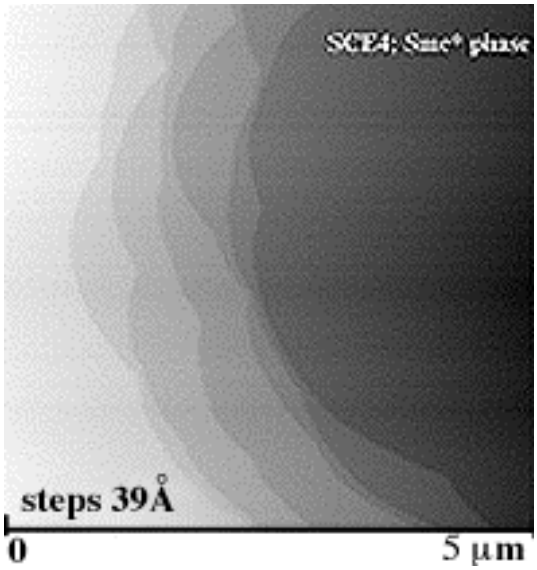

Fig. 10. Terraces on the bord of a hole in a film transferred by the Maclennan method.

The typical images are shown in Figures 9 and 10. Unfortunately, we were unable to find on them any signature of the 2π disclinations. However, we remarked at once that all transferred films contained a lot of small holes. The depth of these holes was close to the thickness of the transferred films and the lateral size of the order of several tenths of microns. These holes are well visible in an optical microscope so that one can make an estimate of their total surface area which corresponds to about 5% of the area of the transferred film. As it is shown in Figure 10, the edges of holes have most of the time a terrace-like texture allowing to count smectic layers one by one. It is important to emphasise that this topography is characteristic of films transferred by the first stage of the process and is not related to the subsequent evolution of the catenoid-shaped film.

The most plausible explanation of the presence of these holes in transferred films is that during the first stage of the transfer process, the smectic films must, for geometrical reasons, increase their surface area. Moreover, the rate of the surface change dS/dt must be so high that the transfer of molecules from the meniscus into the film cannot compensate the increase in the film tension [1] resulting from the positive change in its area. Consequently, holes are nucleated in the film. In order to understand better the mechanism of creation of the holes, we calculated the change $\Delta S = S_a - S_b$ in the surface area of smectic films as a function of the distance h between the circular frame and the substrate. These results are presented in the next section.

3 Theoretical

3.1 Surfaces of constant mean curvature

The free film spanned between the circular frame and the flat substrate has the shape of a surface of revolution that can be parametrised as follows (Fig. 3):

$$\mathbf{r}(z,\varphi) = [r(z)\cos\varphi, r(z)\sin\varphi, z]. \tag{1}$$

The principal curvatures of such a surface are [7]

$$k_1 = -\frac{\begin{vmatrix} 1 & r' \\ 0 & r'' \end{vmatrix}}{(1+r'^2)^{3/2}} \tag{2}$$

and

$$k_2 = \frac{1}{r(1+r'^2)^{1/2}}\,. \tag{3}$$

The mean curvature of the free film is then

$$M_f = \frac{k_1+k_2}{2} = \frac{1+r'^2-rr''}{2r(1+r'^2)^{3/2}}\,. \tag{4}$$

In the presence of the pressure Δp inside the surface, its equilibrium shape is given by the Laplace condition

$$M_f = \frac{\Delta p}{\tau} \tag{5}$$

where τ is the film tension. In experiments, the applied pressure Δp is such that the top of the spherical cup touches the substrate. In these conditions, the mean curvature M_s of the spherical cup, obtained from simple geometric considerations

$$M_s = \frac{2h}{R^2+h^2} \tag{6}$$

must satisfy the Laplace condition too

$$M_s = \frac{\Delta p}{\tau}\,. \tag{7}$$

By equating M_f and M_s, one gets finally the following differential equation:

$$\frac{1+r'^2-rr''}{2r(1+r'^2)^{3/2}} = \frac{2h}{R^2+h^2} \tag{8}$$

ruling the shape of the free film.

3.2 Change in the surface area during the transfer of films

The equation (8) has been solved numerically and the total surface area S_a (the area of the circular transferred film plus the area of the free film) has been calculated as a function of the distance h (empty circles in the plot of Fig. 11). We have also calculated the surface area S_b of the spherical cap touching the substrate (empty triangles in the plot of Fig. 11). It is obvious from these two plots that the difference between S_a and S_b increases with h. As mentioned in Section 2, this change $\Delta S = S_a - S_b$ in the surface area takes place in a few milliseconds and, therefore, results in an increase of the film tension that generates pores visible in AFM.

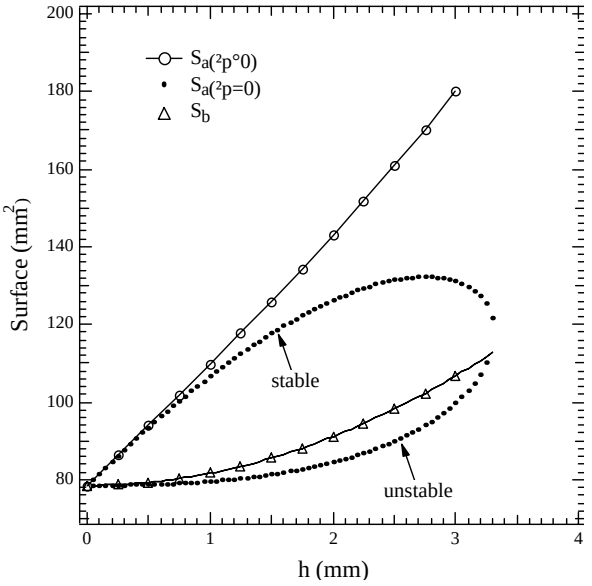

Fig. 11. Comparison between the surface areas of the smectic film before (S_b) and after (S_a) the first stage of the transfer. Surfaces are calculated for the circular aperture of radius $R =$ 5 mm.

We extended our calculations of the surface area S_a to the case of zero differential pressure. The corresponding plot in Figure 11 (dots) has two branches corresponding to the stable and unstable forms of the catenoid. Let us remark that for a given distance h, the surface area S_a is larger in the presence of the pressure Δp then in the absence of the pressure. This result is in agreement with experimental results concerning the second stage of the transfer process; when the pressure is increased, the surface area as well as the radius r_0 of the free film increase. Obviously, the surface area πr_0^2 of the substrate covered with the liquid crystal increases too.

The shapes of the free-standing film created after the first stage of the transfer process ($\Delta p_0 = \text{const}$) have been calculated for different values of the distance h. They are shown in Figure 12. It is interesting to note that these shapes evolve as a function of h. For h close to zero, the free-standing film must obviously have a shape close to the catenoid because the pressure Δp_0 goes to zero in the limit $h \to 0$. In this limit, the principal curvatures of the free film are of opposite sign and their absolute values are very close. When the distance h increases, the mean curvature of the surface must increase in order to equilibrate the pressure Δp which grows as $2h/(R^2+h^2)$. This change in the mean curvature is mainly due to the variation of the curvature k_1 which decreases and changes sign for a certain threshold value h_{cyl} of the distance between

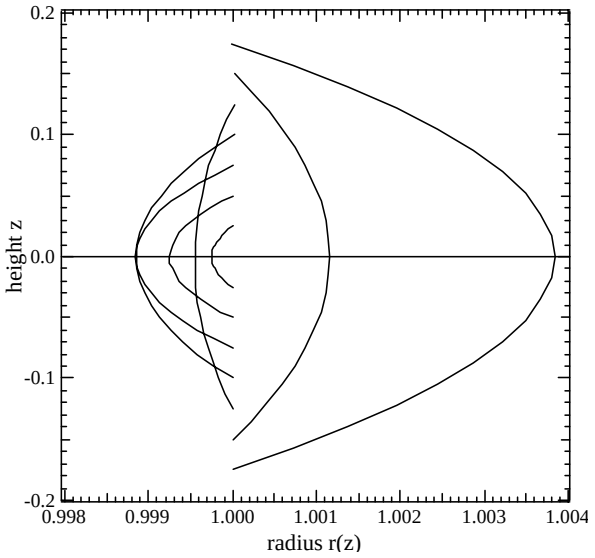

Fig. 12. Shapes $r(z)$ of the free film after the first stage of the transfer. The series of plots corresponds to distances $h = 0.05$, 0.10, 0.15, 0.20, 0.25 and 0.30. Note the difference in scales of $r(z)$ and z.

the substrate and the circular frame. In order to calculate h_{cyl} let us remark that for the cylindrical shape, the generic function $r(z)$ is constant and equal to R. The equation (8) becomes then

$$\frac{1}{2R} = \frac{2h}{R^2 + h^2} \cdot \tag{9}$$

Its root

$$\frac{h_{cyl}}{R} = 2 - \sqrt{3} \approx 0.268 \tag{10}$$

corresponds precisely to the threshold distance h_{cyl}.

3.3 shape of the catenoid

When there is no pressure difference Δp between the two sides of the free film, the right hand side of the equation (8) equals to zero and there exists an analytic solution – the catenoid:

$$r(z) = r_0 \cosh\left(\frac{z}{r_0}\right) \cdot \tag{11}$$

The parameter r_0 represents here the minimal radius of the catenoid at $z = 0$. In experiments with the free film spanned between the circular aperture and the flat substrate (where the contact angle is $\pi/2$), the free film realises one half of the catenoid and r_0 corresponds to the radius of the catenoid at the substrate plate. For $z = h$, the radius $r(h) = R$ so that h and r_0 are related:

$$\frac{R}{r_0} = \cosh\left(\frac{h}{r_0}\right) \cdot \tag{12}$$

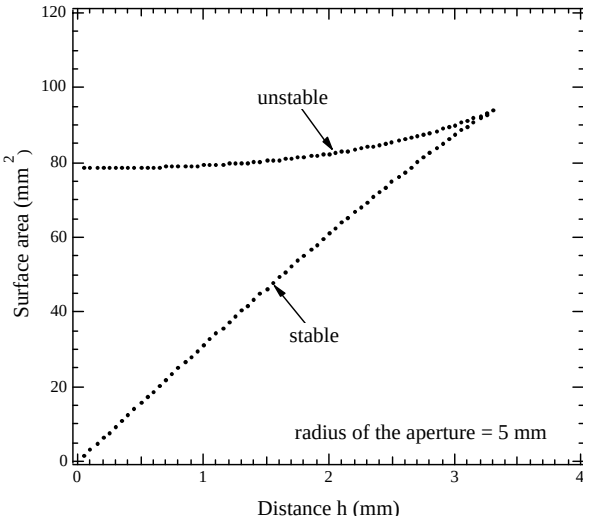

Fig. 13. Surface area of the the stable and unstable forms of the catenoid.

Using R as the unit length and introducing reduced variables $\rho = r_0/R$ and $\chi = H/R$ ($h = H/2$), this equation can be written as:

$$\chi = 2\rho \,\mathrm{arcch}\left(\frac{1}{\rho}\right) \cdot \tag{13}$$

Using this function, continuous lines were plotted in Figures 4, 5 and 8. The function $\chi(\rho)$ is well defined in the range $0 \leq \rho \leq 1$. One has $\chi(\rho) = 0$, for $\rho_1 = 0$ and $\rho_2 = 1$. For $\rho^* = 0.5524$, there is a maximum $\chi^* = 1.3254$. The coordinates (ρ^*, χ^*) of this maximum correspond well to the experimentally measures values $r^* = 2.75$ mm and $h^* = 3.3$ mm. For $0 < \chi < \chi^*$, there are two solutions ρ_1 and ρ_2 corresponding to the stable and unstable forms of the catenoid.

It is interesting to calculate the corresponding surface areas $S_1(h)$ and $S_2(h)$ and to compare them. Knowing the shape $r(z)$ of the surface (Eq. (11)) the function $S(h)$ can be calculated analytically as the integral:

$$S(h) = \int_0^h 2\pi r \sqrt{1 + r'^2} dz \tag{14}$$

and represented in the parametric form:

$$\begin{aligned} S(r_0) &= \pi r_0^2 \left\{ \mathrm{arc\,sinh}\left[\sinh\left(\frac{h}{r_0}\right)\right] \right. \\ &\quad \left. + \cosh\left(\frac{h}{r_0}\right) \sinh\left(\frac{h}{r_0}\right) \right\} \\ h(r_0) &= r_0 \,\mathrm{arc\,cosh}\left(\frac{R}{r_0}\right) \end{aligned} \tag{15}$$

where r_0 has to be varied between 0 and R. The plot $S(h)$ is shown in Figure 13. One remarks that for a given distance h less than the critical one $h^* = \chi^* R/2$, the unstable form of the catenoid has the surface (the capillary energy) larger than the stable form (due to the fact that

the contact angle at the substrate is $\pi/2$, the area πr_0^2 of the surface wetted by the LC does not matter in this comparison of the surface energies). Another interesting feature of this plot is that slopes dS/dh are positive for the two branches. It means that the substrate plate is always attracted toward the aperture. This is not surprising because the force of interaction $dE/dh = \tau(dS/dh)$ resulting from the slope dS/dh, must be equal to the tension of the film τ multiplied by the perimeter $2\pi r_0$ of the film at the substrate. Therefore, one must have:

$$2\pi r_0 = \frac{dS}{dh} \cdot \tag{16}$$

By differentiating numerically the calculated function $S(h)$ shown in Figure 13, we obtained a plot (within the factor 2π) identical with $r_0(h)$ shown in Figure 4.

4 Discussion and conclusions

We have shown here that during the first stage of the Maclennan transfer process, the total surface area of the smectic film increases by an amount ΔS that depends on the distance between the frame and the substrate. As a result, a number of microscopic holes are generated in the transferred film, which thickness, everywhere else, is uniform and corresponds to the one of the free film before the transfer. The number of holes should be reduced by decreasing as much as possible the distance h between the free film and the substrate because ΔS goes linearly to zero with h.

For a given surface area variation ΔS, it is not clear however, how the rate dS/dt of the surface change evolves with time. Indeed, this first stage of the transfer process takes place in a few milliseconds so that in order to resolve its dynamics experimentally a fast enough camera should be used. From theoretical point of view, the dynamics of the transfer process seems quite complex. It is driven by forces of interaction between the free film and the substrate which are unknown so far. It also involves complex flows in air that must be expulsed from the space between the film and the substrate.

During the study of shapes of free films spanned between the substrate and the frame, we have found that in the absence of pressure, two catenoid-like shapes are possible: one stable and the other one unstable. Due to the presence of the meniscus at the substrate plate, the contact angle between the film and the substrate is $\pi/2$.

Let us note that this configuration is different from the one of Debregas and Brochard-Wyart [9] who recently studied shapes of a liquid bridge formed between a free surface of a liquid and a flat substrate parallel to it. Indeed, in experiments presented in [9], the surface of the bridge is submitted to the hydrostatic pressure varying linearly with the height z, while in our case the pressure is independent of z (zero or constant). This difference is crucial in equations ruling the shape of the surface (Eq. (2) in [9] and Eq. (8) here) where the Laplace force due to the local mean curvature is compared with the local pressure. The second difference comes from different boundary conditions, in particular, at the substrate plate where, in the case of reference [9] the contact angle is in general different from $\pi/2$ while in our experiments it is $\pi/2$ due to the presence of the meniscus.

We have shown that thanks to the viscous drag of the meniscus on the substrate, the relaxation time involved in changes of the catenoid parameters is so long (several seconds) that the unstable form of the catenoid can be maintained dynamically by a suitable regulation of the distance h. This is in contrast with the case of a catenoid spanned between two ring-shaped frames where the relaxation time is so short that the unstable form predicted theoretically has never been observed in experiments.

We are grateful to Martine Ben Amar and Patricio da Silva for useful discussions on the geometry and dynamics of minimal surfaces.

References

1. P. Pieranski, L. Beliard, J.-Ph. Tournellec, X. Leoncini, C. Furtlehner, H. Dumoulin, E. Riou, B. Jouvin, J.-P. Fénerol, Ph. Palaric, J. Heuving, B. Cartier, I. Kraus, Physica A **194**, 364 (1993).
2. J. Maclennan, G. Decher, U. Sohling, App. Phys. Lett. **59**, 917 (1991).
3. P. Oswald, J. Phys. France **48**, 897 (1987).
4. S.A. Cryer, P.H. Steen, J. Coll. Int. Sc. **154**, 276 (1992).
5. J. Maclennan, Europhys. Lett. **13**, 435 (1990).
6. E. Demikhov, H. Stegemeyer, Liq. Cryst. **18**, 37 (1995).
7. B. O'Neill, *Elementary differential geometry*, V.6 (Academic Press, 1966).
8. M. Ben Amar, P.P. da Silva, N. Limodin, A. Langlois, M. Brazovskaia, C. Even, V. Chikina, P. Pieranski, *Stability and vibrations of catenoid-shaped smectic films*, accompanying paper.
9. G. Debregeas, F. Brochard-Wyart, J. Coll. Int. Sc. **190**, 134 (1997).